



**UNIVERSITI PUTRA MALAYSIA**

**MODELLING AND SIMULATION OF Si/SiGe  
HETEROSTRUCTURE DEVICES**

**NORULHUDA BT ABD. RASHEID**

**FK 2002 16**

**MODELLING AND SIMULATION OF Si/SiGe HETEROSTRUCTURE  
DEVICES**

**By**

**NORULHUDA BT ABD. RASHEID**

**Thesis Submitted to the School of Graduate Studies, Universiti Putra Malaysia,  
in Fulfilment of Requirement for the Degree of Master of Science**

**April 2002**



*To my beloved family*

*my husband, Mohd Radhwan Abd Karim  
and my children, Farisa Alia, Muhammad Farhan and Ili Rawaida.*

*Thank you for giving me the full support and confidence through out my studies  
and most of all thank you for giving me all the LOVE I need.*

*May ALLAH bless you all... ..Amin*



Abstract of thesis presented to the Senate of Universiti Putra Malaysia in fulfilment  
of the requirements for the degree of Master of Science

**MODELLING AND SIMULATIONS OF THE Si/SiGe  
HETEROSTRUCTURE DEVICES**

**By**

**NORULHUDA BT ABD RASHEID**

**April 2002**

**Chairperson: Roslina bt Mohd Sidek, Ph.D.**

**Faculty: Engineering**

Complementary metal-oxide-semiconductor (CMOS) is currently the most dominant technology used in making integrated systems. It consists of both n-channel MOS transistor (NMOS) and p-channel MOS transistor (PMOS) fabricated on the same substrate. Conventionally, the substrate is made of silicon. Alternatively, the substrate can be made from different layer of semiconductors known as heterostructure. Much attention has been given to Si/SiGe due to its compatibility with silicon and the higher carrier mobilities. SiGe is an alloy which is said to be an alternative solution to the problem of a down-scaled CMOS to produce high speed device.

This work consists of modelling three different of Si/SiGe heterostructure substrates which are used to construct n- and p-channel MOSFETs and later to construct CMOS inverter. The three types of heterostructures are a strained SiGe on silicon substrate, a strained silicon on relaxed SiGe/Si substrate and a strained SiGe on strained Si/relaxed layers of SiGe/Si substrate.



A device simulator, Avanti MEDICI Version 1999.2 is used in this project. Although it has heterojunction capability, it does not support model for a strained Si. This work also highlights the method to simulate Si/SiGe heterostructures containing strained layer using MEDICI. Simulations on the band structure and current-voltage (I-V) characteristics of the MOSFETs are carried out. The  $I_d-V_g$  and  $I_d-V_d$  are simulated for different value of Ge% and mobility. This is to observe the effect of varying the value of Ge% and mobility used in the design. The simulation on the CMOS inverter as the fundamental circuit is carried out to obtain the transfer curve. The noise margin and switching characteristics can be extracted from the transfer curve.

All the simulated results are then compared with the Si bulk. The analyses show that the performance of the Si/SiGe heterostructures is better in terms of the electrical characteristics of the MOSFETs and the switching characteristics of the CMOS inverter, as compared to the performance of the Si bulk.



Abstrak tesis yang dikemukakan kepada Senat Universiti Putra Malaysia sebagai memenuhi keperluan untuk ijazah Master Sains

## **MODEL DAN SIMULASI PERANTI-PERANTI SIMPANG-HETERO Si/SiGe**

Oleh

**NORULHUDA BT ABD RASHEID**

April 2002

**Pengerusi: Roslina bt Mohd Sidek, Ph.D.**

**Fakulti: Kejuruteraan**

Semikonduktor-oksida-logam pelengkap (CMOS) adalah teknologi dominasi terkini dalam membuat sistem bersepadu. Ia terdiri daripada transistor MOS saluran n (NMOS) dan transistor MOS saluran p (PMOS) yang difabrikasikan di atas substrat yang sama. Kebiasaannya, substrat diperbuat daripada silikon. Secara pilihan, substrat boleh juga dibuat daripada lapisan semikonduktor yang berlainan yang dikenali sebagai struktur-hetero. Perhatian yang banyak telah diberikan kepada struktur-hetero Si/SiGe kerana keserasiannya dengan silikon dan mobiliti-mobiliti pembawa yang tinggi. SiGe adalah sejenis aloi yang dikatakan sebagai salah satu penyelesaian terhadap masalah pengecilan CMOS dalam menghasilkan peranti yang berkelajuan tinggi.

Projek ini mengandungi pemodelan tiga jenis struktur-hetero Si/SiGe yang akan digunakan untuk membina saluran n dan p dan kemudian untuk membina pembalik CMOS. Tiga jenis struktur-hetero tersebut adalah SiGe tegang di atas substrat silikon, silikon tegang di atas lapisan rehat SiGe/substrat Si dan SiGe tegang di atas lapisan silikon tegang/lapisan-lapisan rehat SiGe/substrat Si.



Alat simulasi peranti, Avanti MEDICI Versi 1999.2 digunakan untuk mensimulasikan struktur jalur dan ciri-ciri arus-voltan MOSFET. Walaupun mempunyai keupayaan simpang-hetero, ia tidak menyokong model untuk silikon tegang. Cara-cara untuk mensimulasikan struktur-hetero Si/SiGe yang mempunyai lapisan silikon tegang dengan menggunakan MEDICI diketengahkan di dalam tesis ini. Simulasi dijalankan ke atas struktur jalur dan ciri-ciri arus-voltan (I-V) MOSFET.  $I_d-V_g$  dan  $I_d-V_d$  disimulasikan bagi nilai Ge% dan mobiliti yang berbeza. Ini adalah bertujuan untuk memerhati kesan perubahan nilai Ge% dan mobiliti dalam rekabentuk tersebut. Simulasi ke atas pembalik CMOS sebagai litar asas dijalankan untuk mendapatkan lengkung pindah. Jidar hingar dan ciri-ciri suis boleh didapati daripada lengkung pindah tersebut.

Keputusan-keputusan simulasi kemudian dibandingkan dengan Si pukal. Analisis-  
analisis menunjukkan bahawa pencapaian bagi simpang-hetero Si/SiGe adalah lebih baik jika dibandingkan dengan pencapaian bagi Si pukal, dari segi ciri-ciri elektrik MOSFET dan ciri-ciri suis pembalik CMOS.



## ACKNOWLEDGEMENTS

I would like to express my sincere gratitude to my project supervisor, Dr. Roslina bt Mohd Sidek, for the generous encouragement and guidance from the beginning of the project to the completion of this thesis.

Other deserving thanks include Norhazlin bt Jalalludin, the research assistant to Dr. Roslina, who has taught me to use the device simulator, MEDICI. Also, I would like to thank the other supervisory committee members, Encik Rahman Wagiran and Encik Nasri for the valuable comments and guidance.



## TABLE OF CONTENTS

	<b>Page</b>
DEDICATION	ii
ABSTRACT	iii
ABSTRAK	v
ACKNOWLEDGEMENTS	vii
APPROVAL SHEETS	viii
DECLARATION FORM	x
LIST OF TABLES	xiii
LIST OF FIGURES	xv
LIST OF ABBREVIATIONS	xx
<b>CHAPTER</b>	
1 INTRODUCTION	
1.1 The advantage of CMOS	2
1.2 Limitations of Down-Scaled CMOS	3
1.3 Silicon Germanium (SiGe)	3
1.4 The advantage of Si/SiGe	4
1.5 Objectives	5
1.6 Thesis Structure	5
2 LITERATURE REVIEW	
2.1 Properties of Silicon Germanium (SiGe)	7
2.1.1 Misfit Dislocation and Critical Thickness in SiGe	7
2.1.2 Energy Gap and Band Structure of SiGe	13
2.1.2.1 Strained Silicon Formed on Bulk $\text{Si}_{1-x}\text{Ge}_x$	13
2.1.2.2 Strained $\text{Si}_{1-x}\text{Ge}_x$ Formed on Bulk Silicon	14
2.1.3 Hole Mobilities In Strained SiGe.	15
2.1.4 Electron Mobility in Strained Silicon	15
2.2 Avanti MEDICI Device Simulator	17
2.2.1 MEDICI Input Statements	17
2.3 Heterojunction Device Advanced Application Module (HD-AAM) Used with MEDICI	20
2.3.1 Material Parameters	20
2.3.2 Energy Bandgap Models	20
2.3.3 Mobility Models	22
2.3.4 Grid in MEDICI	23
2.4 The Structure of The Si/SiGe MOSFETs	24
2.5 CMOS Inverter	30
2.5.1 DC Analysis	30
2.5.2 Transient Analysis	34
2.6 Conclusion	36



3	METHODOLOGY	
3.1	Construction of the Si/SiGe Based NMOS and PMOS Structures	37
3.1.1	Construction of the Si Bulk MOSFET	42
3.2	Verification of Band Structure	43
3.3	I-V Characteristics of MOSFETs	45
3.3.1	Gate Characteristic	45
3.3.2	Drain Characteristic	46
3.4	CMOS Inverter	47
3.5	Simulation Flow Chart for The Three Substrate Structures	50
4	RESULTS AND DISCUSSION	
4.1	Construction of SiGe MOSFET	51
4.2	Verification of Band Structure	53
4.2.1	Strained SiGe on Si Substrate	53
4.2.2	Strained Si on Relaxed SiGe	59
4.2.3	Strained SiGe on Strained Si	60
4.2.4	Si Bulk	62
4.3	I-V Characteristics	63
4.3.1	Strained SiGe on Si Substrate	63
4.3.1.1	Gate Characteristics	63
4.3.1.2	Drain Characteristics	68
4.3.2	Strained Si on Relaxed SiGe	73
4.3.2.1	Gate Characteristics	73
4.3.2.2	Drain Characteristics	75
4.3.3	Strained SiGe on Strained Si	77
4.3.3.1	Gate Characteristics	77
4.3.3.2	Drain Characteristics	80
4.3.4	Si Bulk	81
4.4	CMOS Inverter Circuit	82
4.4.1	Strained SiGe on Si Substrate	82
4.4.2	Strained Si on Relaxed SiGe	87
4.4.3	Strained SiGe on Strained Si	88
4.4.4	Si Bulk	89
5	CONCLUSION	
5.1	Conclusion	90
5.2	Further Work	91
	REFERENCES	92
	APPENDICES	95
	BIODATA OF THE AUTHOR	118



## LIST OF TABLES

Table		Page
1	Mobility choices in Medici	23
2	Material parameters on relaxed Si <sub>0.7</sub> Ge <sub>0.3</sub> buffer	42
3	The simulated and calculated values of the band energies for different values of the Ge mole fraction in the SiGe PMOS	58
4	The simulated and calculated values of the band energies for different values of the Ge mole fraction in the SiGe NMOS	58
5	The simulated and calculated values of the band energies with the Ge mole fraction, Ge=30% in the SiGe NMOS	60
6	The simulated and calculated values of the band energies with the Ge mole fraction, Ge=30% in the SiGe PMOS	60
7	Band energy values at different carrier mobilities and fixed Ge mole fraction at Ge=30%	61
8	The threshold voltage values for different value of the Ge mole fraction and fixed hole mobility at $\mu_e(\text{Si}) = 600 \text{ cm}^2/\text{Vs}$ , $\mu_e(\text{SiGe}) = 600 \text{ cm}^2/\text{Vs}$ , $\mu_h(\text{Si}) = 600 \text{ cm}^2/\text{Vs}$ and $\mu_h(\text{SiGe}) = 600 \text{ cm}^2/\text{Vs}$	65
9	The threshold voltage values for different value of the hole mobility in the SiGe layer and fixed Ge mole fraction at Ge=30%	67
10	The saturated drain current values for different value of the Ge mole fraction and fixed hole mobility at $\mu_e(\text{Si}) = 600 \text{ cm}^2/\text{Vs}$ , $\mu_e(\text{SiGe}) = 600 \text{ cm}^2/\text{Vs}$ , $\mu_h(\text{Si}) = 600 \text{ cm}^2/\text{Vs}$ and $\mu_h(\text{SiGe}) = 600 \text{ cm}^2/\text{Vs}$	69
11	The saturated drain current values for different value of the hole mobility in the SiGe layer and fixed Ge mole fraction at Ge=30%	72
12	The threshold voltage values of the SiGe MOSFET and the Si bulk MOSFET	74



13	The saturated drain current values of the SiGe MOSFET and the Si bulk MOSFET	76
14	The I-V characteristics of the Si bulk	81
15	CMOS inverter performance at different value of the Ge mole fraction and fixed hole mobility at $\mu_h=600 \text{ cm}^2/\text{Vs}$ using $n^+$ -polysilicon gate	84
16	CMOS inverter performance at different value of the Ge mole fraction and fixed hole mobility at $\mu_h=600 \text{ cm}^2/\text{Vs}$ using $p^+$ -polysilicon gate	85
17	CMOS inverter performance at different hole mobility and fixed Ge mole fraction at Ge=30% using $n^+$ -polysilicon gate	85
18	CMOS inverter performance at different hole mobility and fixed Ge mole fraction at Ge=30% using $p^+$ -polysilicon gate	86
19	The inverter performance of the SiGe CMOS and Bulk CMOS	88
20	CMOS inverter performance at various carrier mobility values and fixed Ge mole fraction at Ge=30%	88
21	Si bulk CMOS inverter performance	89



## LIST OF FIGURES

Figure		Page
1.1	Cross-section of CMOS.	1
2.1	Atomic structure of relaxed SiGe and Si bulk	8
2.2	Structure of SiGe grown below the critical thickness	8
2.3	Misfit Dislocation due to the grown SiGe above the critical thickness	9
2.4	Critical thickness for SiGe on bulk unstrained Si as a function of Ge concentration	10
2.5	A structure of strained silicon on a relaxed Si <sub>1-x</sub> Ge <sub>x</sub> below the critical thickness	11
2.6	Structure of the strained Si <sub>1-x</sub> Ge <sub>x</sub> on strained Si below the critical thickness	12
2.7	The band gap of strained Si on Si <sub>1-x</sub> Ge <sub>x</sub> buffer	13
2.8	The band gap of strained Si <sub>1-x</sub> Ge <sub>x</sub> on Si buffer	14
2.9	Band diagram with two different materials forming a heterojunction	21
2.10	Schematic cross section of the Si/SiGe layer structure	24
2.11	Fundamental indirect energy gap of strained Si <sub>1-x</sub> Ge <sub>x</sub> alloys in comparison with the bulk alloy	28
2.12	(a) Schematic device cross-section of a strained SiGe p-MOSFET (b) Band diagram of this device when the device is 'ON'	29
2.13	(a) CMOS inverter circuit diagram (b) CMOS inverter transfer characteristic	32
2.14	CMOS inverter noise margin	32
3.1	MOSFET with strained SiGe on relaxed Si substrate	38
3.2	MOSFET with strained Si on relaxed SiGe	39
3.3	MOSFET with strained Si on strained SiGe	39



3.4	Si bulk MOSFET	43
3.5	The band gap of strained Si <sub>0.7</sub> Ge <sub>0.3</sub> on Si bulk	44
3.6	The band gap of strained Si on relaxed Si <sub>0.7</sub> Ge <sub>0.3</sub>	45
3.7	The I <sub>D</sub> – V <sub>GS</sub> characteristic to determine V <sub>T</sub>	46
3.8	Drain characteristics	47
3.9	Pulse waveform used in transient simulation	48
3.10	Schematic diagram of the two identical CMOS inverter circuits	49
3.11	Simulation flow chart for the three substrate structures	50
4.1	Doping regrid of the SiGe MOSFET	51
4.2	The schematic substrate structure of the strained SiGe on Si	52
4.3	The schematic substrate structure of the strained Si on relaxed SiGe	52
4.4	The schematic substrate structure of the strained SiGe on strained Si	53
4.5(a)	Band diagram of the SiGe PMOS at Ge=30%	54
4.5(b)	Band diagram of the SiGe NMOS at Ge=30%	54
4.6(a)	Band diagram of the SiGe PMOS at Ge=50%	55
4.6(b)	Band diagram of the SiGe NMOS at Ge=50%	55
4.7	The effect of the gate material on the band diagram of the SiGe PMOS	56
4.8	The effect of the gate material on the band diagram of the SiGe NMOS	56
4.9(a)	Band diagram of the SiGe PMOS with different hole mobilities in the SiGe layer and fixed Ge mole fraction at Ge=30%	57

4.9(b)	Band diagram of the SiGe NMOS with different hole mobilities in the SiGe layer and fixed Ge mole fraction at Ge=30%	57
4.10	Band diagram of the SiGe NMOS at Ge=30%	59
4.11	Band diagram of the SiGe NMOS at Ge=30%	61
4.12	Gate characteristic of the SiGe PMOS with different Ge mole fraction, $\mu_e(\text{Si}) = 600 \text{ cm}^2/\text{Vs}$ , $\mu_e(\text{SiGe}) = 600 \text{ cm}^2/\text{Vs}$ , $\mu_h(\text{Si}) = 600 \text{ cm}^2/\text{Vs}$ and $\mu_h(\text{SiGe}) = 600 \text{ cm}^2/\text{Vs}$	63
4.13	Gate characteristic of the SiGe NMOS with different Ge mole fraction, $\mu_e(\text{Si}) = 600 \text{ cm}^2/\text{Vs}$ , $\mu_e(\text{SiGe}) = 600 \text{ cm}^2/\text{Vs}$ , $\mu_h(\text{Si}) = 600 \text{ cm}^2/\text{Vs}$ and $\mu_h(\text{SiGe}) = 600 \text{ cm}^2/\text{Vs}$	64
4.14	The effect of the gate material on the gate characteristic of the SiGe PMOS	65
4.15	The effect of the gate material on the gate characteristic of the SiGe NMOS	66
4.16	Gate characteristics of the SiGe PMOS with different hole mobilities in the SiGe layer and fixed Ge mole fraction at Ge=30%	66
4.17	Gate characteristics of the SiGe NMOS with different hole mobilities in the SiGe layer and fixed Ge mole fraction at Ge=30%	67
4.18	Drain characteristic of the SiGe PMOS with different Ge mole fraction, fixed hole mobility at $\mu_E(\text{Si}) = 600 \text{ cm}^2/\text{Vs}$ , $\mu_E(\text{SiGe}) = 600 \text{ cm}^2/\text{Vs}$ , $\mu_h(\text{Si}) = 600 \text{ cm}^2/\text{Vs}$ and $\mu_h(\text{SiGe}) = 600 \text{ cm}^2/\text{Vs}$	68
4.19	Drain characteristic of the SiGe NMOS with different Ge mole fraction and fixed mobility at $\mu_e(\text{Si}) = 600 \text{ cm}^2/\text{Vs}$ and $\mu_e(\text{SiGe}) = 600 \text{ cm}^2/\text{Vs}$ , $\mu_h(\text{Si}) = 600 \text{ cm}^2/\text{Vs}$ and $\mu_h(\text{SiGe}) = 600 \text{ cm}^2/\text{Vs}$	68
4.20	The effect of the gate material on the drain characteristic of the SiGe PMOS	70
4.21	The effect of the gate material on the drain characteristic of the SiGe NMOS	70



4.22	Drain characteristics of the SiGe PMOS with different hole mobilities in the SiGe layer and fixed Ge mole fraction at Ge=30%	71
4.23	Drain characteristics of the SiGe NMOS with different hole mobilities in the SiGe layer and fixed Ge mole fraction at Ge=30%	72
4.24	Gate characteristic of the SiGe NMOS at Ge=30%, $\mu_e(\text{Si}) = 2400 \text{ cm}^2/\text{Vs}$ and $\mu_h = 800 \text{ cm}^2/\text{Vs}$	73
4.25	Gate characteristic of the SiGe PMOS at Ge=30%, $\mu_e(\text{Si}) = 2400 \text{ cm}^2/\text{Vs}$ and $\mu_h = 800 \text{ cm}^2/\text{Vs}$	74
4.26	Drain characteristic of the SiGe NMOS at Ge=30%, $\mu_e(\text{Si}) = 2400 \text{ cm}^2/\text{Vs}$ and $\mu_h = 800 \text{ cm}^2/\text{Vs}$	75
4.27	Drain characteristic of the SiGe PMOS at Ge=30%, $\mu_e(\text{Si}) = 2400 \text{ cm}^2/\text{Vs}$ and $\mu_h = 800 \text{ cm}^2/\text{Vs}$	76
4.28	Gate characteristic of the SiGe NMOS at $\mu_e = 2000 \text{ cm}^2/\text{Vs}$ & $\mu_h = 600 \text{ cm}^2/\text{Vs}$ , $\mu_e = 2200 \text{ cm}^2/\text{Vs}$ & $\mu_h = 800 \text{ cm}^2/\text{Vs}$ , $\mu_e = 2400 \text{ cm}^2/\text{Vs}$ & $\mu_h = 1000 \text{ cm}^2/\text{Vs}$	77
4.29	Gate characteristic of the SiGe PMOS at $\mu_e = 2000 \text{ cm}^2/\text{Vs}$ & $\mu_h = 600 \text{ cm}^2/\text{Vs}$ , $\mu_e = 2200 \text{ cm}^2/\text{Vs}$ & $\mu_h = 800 \text{ cm}^2/\text{Vs}$ , $\mu_e = 2400 \text{ cm}^2/\text{Vs}$ & $\mu_h = 1000 \text{ cm}^2/\text{Vs}$	78
4.30	Electron confinement versus gate bias	79
4.31	Hole confinement versus gate bias	79
4.32	Drain characteristic of the SiGe NMOS at $\mu_e = 2000 \text{ cm}^2/\text{Vs}$ & $\mu_h = 600 \text{ cm}^2/\text{Vs}$ , $\mu_e = 2200 \text{ cm}^2/\text{Vs}$ & $\mu_h = 800 \text{ cm}^2/\text{Vs}$ , $\mu_e = 2400 \text{ cm}^2/\text{Vs}$ & $\mu_h = 1000 \text{ cm}^2/\text{Vs}$	80
4.33	Drain characteristic of the SiGe PMOS at $\mu_e = 2000 \text{ cm}^2/\text{Vs}$ & $\mu_h = 600 \text{ cm}^2/\text{Vs}$ , $\mu_e = 2200 \text{ cm}^2/\text{Vs}$ & $\mu_h = 800 \text{ cm}^2/\text{Vs}$ , $\mu_e = 2400 \text{ cm}^2/\text{Vs}$ & $\mu_h = 1000 \text{ cm}^2/\text{Vs}$	81
4.34	The CMOS inverter transfer curve at Ge=30% and fixed hole mobility at $\mu_h = 600 \text{ cm}^2/\text{Vs}$ using $n^+$ -polysilicon gate	83
4.35	The CMOS inverter transfer curve at Ge=50% and fixed hole mobility at $\mu_h = 600 \text{ cm}^2/\text{Vs}$ using $n^+$ -polysilicon gate	83
4.36	The effect of gate material on CMOS inverter transfer characteristic	84



4.37	Graph of the $V_{out}$ and $V_{in}$ versus time to determine the delay of one CMOS inverter	86
4.38	Graph of the $V_{out}$ and $V_{in}$ versus time to determine the delay of two identical CMOS inverters	87
1	Band diagram of the NMOS	114
2	Band diagram of the PMOS	114
3	Gate characteristic of the NMOS	115
4	Gate characteristic of the PMOS	115
5	Drain characteristic of the NMOS	116
6	Drain characteristic of the PMOS	116
7	Transfer characteristic of the CMOS	117
8	The chain CMOS inverter delay	117



## LIST OF ABBREVIATIONS

MOSFET	Metal-Oxide-Semiconductor Field Effect Transistor
MESFET	Metal-Semiconductor Field Effect Transistor
MODFET	Modulation-Doped Field Effect Transistor
NMOS	n-channel Metal-Oxide-Semiconductor
PMOS	p-channel Metal-Oxide-Semiconductor
CMOS	Complementary Metal-Oxide-Semiconductor
SiGe	Silicon-germanium
$V_T$	Threshold voltage
$I_{Dsat}$	Saturated drain current
$\mu_e$	Electron mobility
$\mu_h$	Hole mobility
$E_g$	Energy gap
$E_V$	Valence band energy
$E_C$	Conduction band energy
$V_{dd}$	Supply voltage
I-V	Current-voltage
$NM_L$	Low noise margin
$NM_H$	High noise margin
$V_{IH}$	High input voltage
$V_{IL}$	Low input voltage
$V_{OH}$	High output voltage
$V_{OL}$	Low output voltage



## CHAPTER 1

### INTRODUCTION

Complementary metal-oxide-semiconductor (CMOS) consists of both n-channel MOS (NMOS) and p-channel MOS (PMOS) transistors fabricated on the same substrate as shown in Figure 1.1 [1].

Since the early eighties until today, complementary metal-oxide-semiconductor (CMOS) has emerged as the dominant technology for general purpose integrated circuit applications [2]. As trend continues, CMOS has edged out less competitive technologies such as bipolar and NMOS, while relegating more exotic technologies such as GaAs to niche applications.

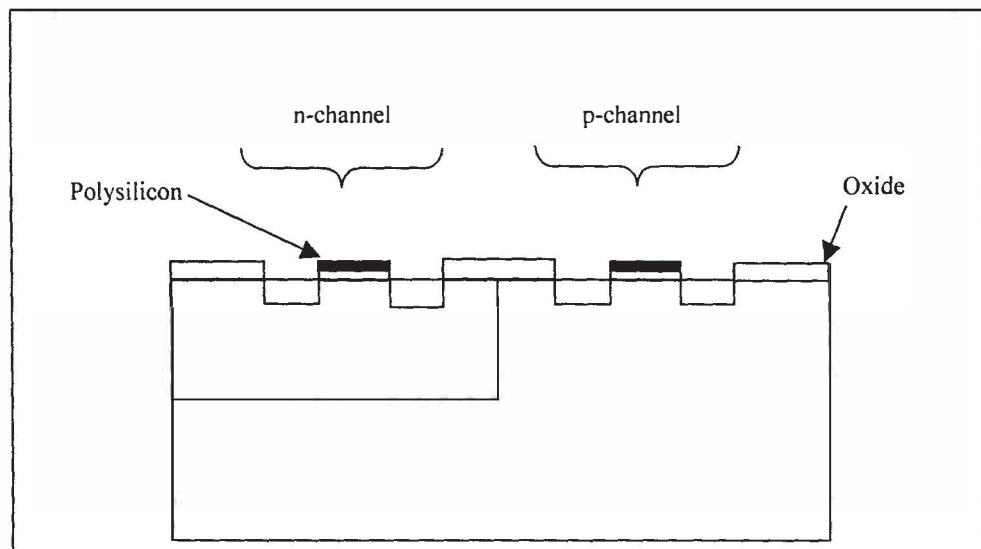


Figure 1.1: Cross-section of CMOS

## 1.1 The Advantage of CMOS

CMOS is recognized as a leading contender for existing and future VLSI systems. Since the beginning of VLSI era, CMOS technology has gained more and more significance than its predecessor: the NMOS technology. There are several main reasons, which has contributed to the use and acceptance of the CMOS technology [3]. CMOS circuits have been at the forefront of the technology primarily due to their passive power consumption. Aside from leakage currents, power in digital circuits are dissipated only during switching events. There is virtually no power consumed when the circuit is in steady state.

Another significant feature of CMOS is its stability of operation. Unlike its counterpart technologies such as NMOS and bipolar, small deviation in device characteristics do not perturb the circuit operating point. It has proven to be robust and permits large quantities and varieties of ICs to be fabricated with high yield.

CMOS is flexible for a wide variety of applications, which includes digital logic, static/dynamic random access memories (RAMs), signal processing and a variety of analogue circuits. As a result, CMOS technology has reached the enviable position where supply generates its own demand. The wide applicability of CMOS has given rise to a broad, high quality infrastructure for development and fabrication that allows advances to be made widely available at a reasonable cost.

In the CMOS circuit, the p-channel transistor has lower performance compared with

n-channel transistor because of the lower mobility of holes than the electrons. However, the performance difference between PMOS and NMOS has reduced drastically due to velocity saturation thus making CMOS technology more attractive in VLSI circuit. CMOS also has another advantage, which is a very large noise margin [4].

## **1.2 Limitations of Down-Scaled CMOS**

From 1960's until now, speed improvement is achieved through down scaling. There are some physical limitations due to down scaling such as the gate oxide becomes very thin ( $\sim 30 \text{ \AA}$ ), the source and drain resistances become more dominating and other parasitic effects. This will reduce the reliability of the device. This is where SiGe alloy is introduced as an alternative solution to produce high speed device.

## **1.3 Silicon Germanium (SiGe)**

A few years after the invention of the bipolar transistor the basic electronic semiconductor material changed from germanium to silicon. During that switch around 1960 considerable interest was focused on bulk, unstrained SiGe alloys. Advance epitaxy methods have enabled the growth of high quality, thin, strained SiGe layers on Si substrates since around 1985 [5]. The availability of strained SiGe/Si structures stimulated heavily the research on silicon-based heterostructure devices resulting within a few years in the fastest silicon-based transistors and other very attractive options.

#### 1.4 The Advantage of Si/SiGe

There have been suggestions to use complementary heterostructure field-effect transistors based on GaAs/AlGaAs in order to make use of the high electron mobility in this material system [6]. However, the problem of the low mobility which plagues Si was not solved. In addition, that technology relied on making Schottky gates, which result in several orders of magnitude higher gate leakage current than in oxide-gated devices.

Unlike the other group III–V elements (e.g. GaAs), SiGe is compatible with silicon process. The intrinsic advantage of Si/SiGe allowing the high-speed operation of the transistors at lower supply voltage would, in principle, result in higher reliability. Although it is inconceivable that Si/SiGe Heterojunction CMOS (HCMOS) will replace Si CMOS in ULSI applications in the near future, there is increasing interest in application-specific designs which require low power consumption and high speed (e.g., cellular phones, other portable electronics, optoelectronic receivers, etc.) [6]. This is where we believe that there is ample room for implementing Si/SiGe HCMOS, making use of its potential performance leverage over Si CMOS.

If cryogenic applications become of importance, the advantage of Si/SiGe over Si will become even more clear, since at 77 K for instance, the electron and hole mobilities are an order of magnitude higher than in Si.